



Journal of Mining and Environment (JME)
journal homepage: www.jme.shahroodut.ac.ir



Mechanism of Zinc Complexation by Alkaline Ligands: A Molecular Modelling Study

Davood Alavi, Sima Mohammadnejad* and Mohammad Javad Koleini

Mineral Processing, Engineering, Tarbiat Modares University, Tehran, Iran

Article Info

Received 21 November 2021

Received in Revised form 27 April 2022

Accepted 5 May 2022

Published online 5 May 2022

DOI: [10.22044/jme.2022.11417.2123](https://doi.org/10.22044/jme.2022.11417.2123)

Keywords

Zinc oxide

Alkaline leaching

Molecular modelling

Smithsonite

Ammonia

Abstract

In this work, the mechanism of zinc hydroxide and ammine complexation in caustic and ammonia leaching is investigated by molecular modelling using the density functional theory method. The speciation of zinc complexes is defined based on the thermodynamic data and Pourbiax diagrams. The mechanism of Zn^{+2} complexation by hydroxide and ammine ligands is simulated by molecular modeling. The structure of reactants in the form of individual clusters is modelled using the density function theory. In order to compare the hydroxide and ammine species structures, the geometry studies are carried out as well. The ammoniacal salt effectiveness to improve the dissolution and stability of the ammine species is studied. The ligand single molecule interaction with a smithsonite molecule is done for a better understanding. Molecular modeling show that the zinc hydroxide species are more stable based on the higher reaction free energies. The reaction free energies decrease by adding the OH^- and NH_3 ions to the complexes from -30.12 kcal/mol to -16.943 kcal/mol, and -22.590 kcal/mol to 66.516 kcal/mol, respectively. The $Zn-OH$ bonds are shorter than $Zn-NH_3$, and the ammine species show more regular structures in comparison with the hydroxide structures. The change of free energies in the presence of ammoniacal salts indicate that the sulfate ions can significantly improve the dissolution of zinc oxide in ammonia. The smithsonite interaction with ammonia and hydroxide reveal that hydroxide ions lead to a higher interaction energy than ammonia (-36.396 vs. -28.238), which is consistent with the higher stability of hydroxide species. The results obtained well-explain the experimental results obtained before, and can be effectively used to optimize the alkaline leaching of zinc oxide ore.

1. Introduction

Zinc oxide minerals such as hemimorphite and smithsonite are alternative sources for zinc production, as high-grade sulfide deposits have been depleted significantly in the last few decades [1, 2]. Hydrometallurgy is the most common method for extraction of zinc from oxide ores [3].

Several leaching agents have been used for dissolution of zinc in oxide ores including inorganic acids as the most common reagent [2, 4, 5] and organic acids [6-8]. Furthermore, the alkaline treatment of low-grade zinc oxide ores has received a lot of attention in the recent years [9-13].

Alkaline leaching mostly by ammonia and soda has a lot of benefits in the hydrometallurgical

extraction of zinc [14-17]. The impurities such as Fe, Cu, Cd, Co, and Ni are not leached out in alkaline media, which result in lower reagent consumption. Also zinc solution purification is the most challenging step to produce zinc through hydrometallurgical processes. In alkaline leaching, a higher grade zinc cathode is produced with a lower electricity consumption in the electro-winning process [10]. Another advantage of alkaline leaching is the prevention of passivation layer formation on the particles surface in the presence of carbonate gangue, especially in low-grade zinc oxide ores [1, 18-21]. Also silica gel

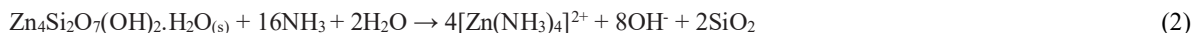
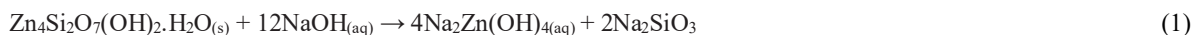
Corresponding author: sima.mnejad@modares.ac.ir (S. Mohammadnejad).

does not form, which is difficult to filtrate and traps zinc in its structure [1, 22].

Dissolution kinetics of alkaline leaching of zinc oxide ores has been studied in recent years for different types of ores. Shrinking core model has been applied for kinetic studies. The alkaline leaching of zinc oxide ores appears both chemically and diffusion control [23-25].

Moreover, the effect of mechanical activation and chelating agents on zinc higher extraction have been investigated [21, 24].

The alkaline dissolution of zinc oxide minerals including smithsonite and hemimorphite is generally described by the following chemical reactions [9, 21]:



Based on the Pourbiax diagram for both zinc ammine and hydroxide, several complexes are stable in varying Eh and pH conditions. For Zn hydroxide, seven $\text{Zn}(\text{OH})_2$, $\text{Zn}(\text{OH})_3^-$, $\text{Zn}(\text{OH})_4^{2-}$, $\text{Zn}(\text{OH})_6^{2-}$, $\text{Zn}_2\text{OH}^{3+}$, $\text{Zn}_4(\text{OH})_4^{4+}$, and ZnOH^+ , and for ammine, four $\text{Zn}(\text{NH}_3)_2^{2+}$, $\text{Zn}(\text{NH}_3)_3^{2+}$, $\text{Zn}(\text{NH}_3)_4^{2+}$, ZnNH_3^+ have been identified. Although alkaline leaching of zinc oxide ores has been the subject of many experimental studies, there are very limited information on the leaching mechanism as well as zinc hydroxide and zinc ammine complexation. Few studies have been performed to understand the mechanism of zinc mineral dissolution in alkaline media based on the leaching residue analysis [23, 26]. However, the spectroscopic studies are subject to many challenges in these meta stable systems as detailed in these investigations. Also the structure of the alkaline complexes is not known, and the factors that affect the stability of these complexes are not researched in details.

Thus the aim of this work is the fundamental study of the mechanism of zinc ammine and hydroxide complexation for the first time to

understand species formation in more details. The obtained results can be efficiently used to interpret the results of the previous experimental studies of zinc oxide minerals leaching in alkaline media.

2. Methods

First of all, for molecular modelling of the species, the zinc hydroxide and ammine species were simulated using the Spana software (free version, 2015). The Eh-pH diagrams were produced for the predominant species complexation. Tables 1 and 2 show the reactions based on the Spana simulations for sodium hydroxide and ammonia leaching, respectively. For simplification and minimization of the calculation cost, the complexation of Zn^{+2} was considered in all models, and the results were obtained without the consideration of intermediate products. Zinc oxide minerals like hemimorphite and willemite had siliceous in their structure; however, siliceous precipitates were shown at rarely high alkalinity as amorphous silica.

Table 1. Zinc hydroxide complexes with stability constants (Spana software).

Eq.	Reactions	LogK
5	$\text{Zn}^{2+} \rightarrow \text{H}^+ + \text{ZnOH}^+$	-8.96
6	$\text{Zn}^{2+} \rightarrow 2\text{H}^+ + \text{Zn}(\text{OH})_2$	-16.9
7	$\text{Zn}^{2+} \rightarrow 3\text{H}^+ + \text{Zn}(\text{OH})_3^-$	-28.4
8	$\text{Zn}^{2+} \rightarrow 4\text{H}^+ + \text{Zn}(\text{OH})_4^{2-}$	-41.2
9	$2\text{Zn}^{2+} \rightarrow \text{H}^+ + \text{Zn}_2\text{OH}^{3+}$	-9.0
10	$4\text{Zn}^{2+} \rightarrow 4\text{H}^+ + \text{Zn}_4(\text{OH})_4^{4+}$	-27.0
11	$2\text{Zn}^{2+} \rightarrow 6\text{H}^+ + \text{Zn}_2(\text{OH})_6^{2-}$	-54.3

Table 2. Zinc amine complexes with stability constants (Spana software).

Eq.	reaction	LogK
12	$\text{Zn}^{2+} + \text{NH}_3 \rightarrow \text{ZnNH}_3^{2+}$	2.21
13	$\text{Zn}^{2+} + 2\text{NH}_3 \rightarrow \text{Zn}(\text{NH}_3)_2^{2+}$	4.5
14	$\text{Zn}^{2+} + 3\text{NH}_3 \rightarrow \text{Zn}(\text{NH}_3)_3^{2+}$	6.86
15	$\text{Zn}^{2+} + 4\text{NH}_3 \rightarrow \text{Zn}(\text{NH}_3)_4^{2+}$	8.89

As Tables 1 and 2 show, by adding more hydroxide and ammonia to the complex structures, the zinc hydroxide and zinc ammonia species became more stable based on LogK.

The reaction mechanism of ammine and hydroxide ions was studied by the molecular modeling simulations. DFT calculations were carried out using the Dmol³ module implemented in Accelrys Materials Studio, version 2017. The zinc, ammine, and hydroxide ions as well as the produced complexes were modelled using the

generalized gradient functional BYLP (exchange functional Becke combined with the Lee–Yang–Parr nonlocal correlation functional) using an Octa-core desktop PC. A double numerical basis set was applied including two atomic orbitals for each occupied orbital for all atoms plus a p-function polarization on hydrogen atoms (DNP) in order to represent hydrogen bonding [27]. The convergence criteria for geometry optimizations are summarized in Table 3.

Table 3. Convergence tolerances for geometry optimization calculations.

Convergence tolerance parameters	Tolerances
Maximum displacement	$5 \times 10^{-4} \text{ \AA}$
Maximum force	$2 \times 10^{-4} \text{ Hartrees/\AA}$
Energy	$1 \times 10^{-6} \text{ Hartrees}$
SCF	10^{-7} Hartrees
Smearing	No
Orbital cut-off	5.0 \AA

No pseudo-potentials or effective core potentials were utilized in this work, and all the results were based on “all electron relativistic” calculations. In order to represent the local environment, calculations were performed using the continuum solvation model, namely COSMO (COnductor like Screening MOdel) [28]. The dielectric constant of water (78.54) was used to outline the solutions in COSMO, presuming a very dilute medium with minor dielectric constant deviation from pure water. Multipolar expansion was used for calculation of the solvation energy for all the models. The geometry optimization was validated based on the vibrational frequency analysis. The geometry structures were considered optimized where there were no negative frequencies.

In order to investigate the feasibility of the reactions, the interaction energy of the reactions was calculated by molecular modeling. For this purpose, the energy difference of each reaction product was calculated from the energy of the reactants. Although the research work indicates that there is a systematic discrepancy between the free energy computed in molecular modeling by this method and the free energy obtained from thermodynamic measurements [29, 30], it can still

serve as a valid basis for comparing the feasibility of different reactions to be used:

$$\Delta G = E_{\text{product}} - E_{\text{reactant}} \quad (16)$$

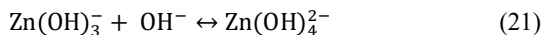
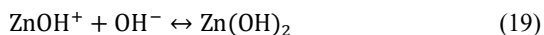
where E_{products} is the total energies of the product clusters, and $E_{\text{reactants}}$ is the total energy of the reactants. The higher negative amounts of ΔG indicate favorable and stronger reaction compared to the positive or lower negative values [31].

3. Results and Discussion

3.1. Zinc leaching mechanism by NaOH

Figure 1 shows the Pourbiach diagram of zinc hydroxide complexes in different Zn concentrations. Based on the Spana thermodynamic simulations, the most stable form of zinc hydroxide in soda leaching in high concentration of NaOH is Zincate ($\text{Zn}(\text{OH})_4^{2-}$). Zincate undergoes Reactions 18-20 by losing OH-groups at a lower pH:





Moreover, the Spana simulations showed that zinc concentration was effective on the other complexes of zinc hydroxide formation and their stability such as Zn(OH)_3^- . As it is evident from

Figure 1, by decreasing the zinc concentration, just zincate appears as a hydroxide complex in the Eh-pH diagrams. These results indicate that zinc could be dissolved by NaOH at potential ranges -1 to 1 V (versus SHE) and at a high pH (above 13).

The zinc hydroxide species were modeled in a molecular scale. Figure 2 shows the zinc hydroxide optimized geometries, and Table 4 presents the free energies of zinc hydroxide complexation resulting from the molecular modeling calculations.

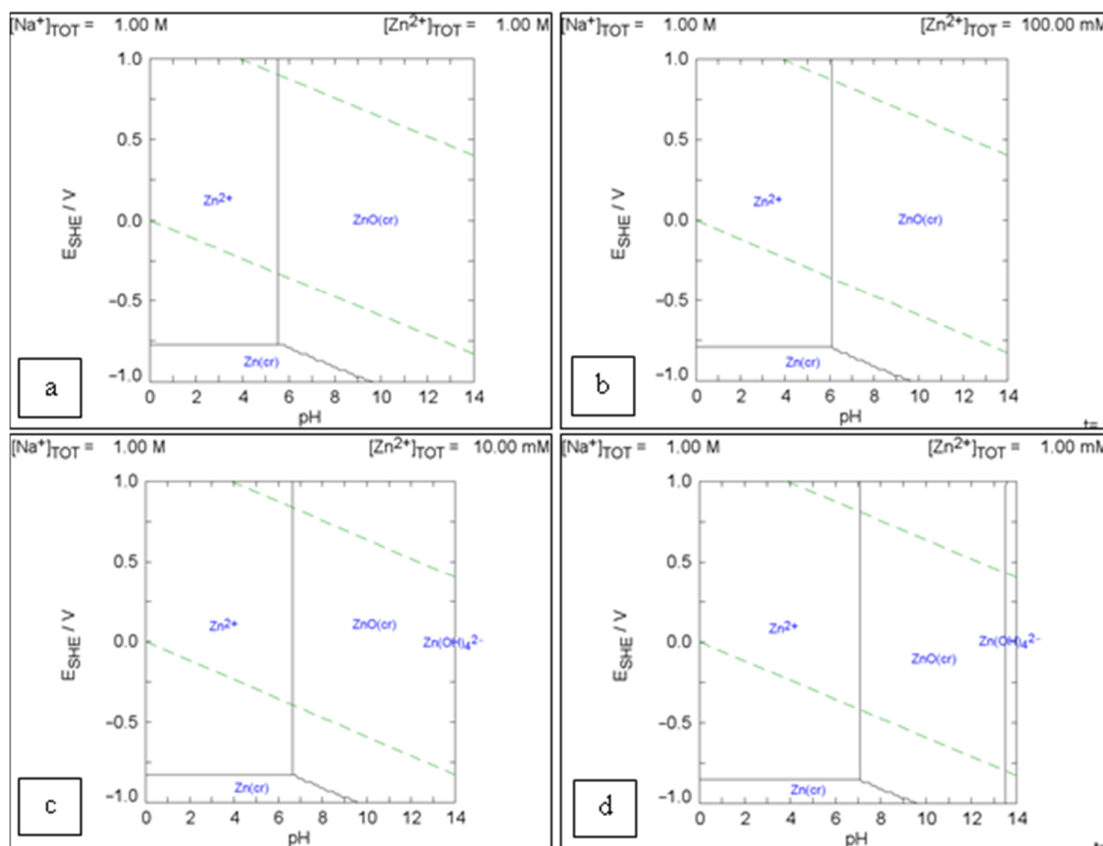


Figure 1. Zinc hydroxide speciation in 25 °C and 1.00 mol of Na^+ (a): $\text{Zn}^{+2} = 1\text{M}$, (b): $\text{Zn}^{+2} = 100$, mM, (c): $\text{Zn}^{+2} = 10$ Mm, and (d): $\text{Zn}^{+2} = 1$ Mm.

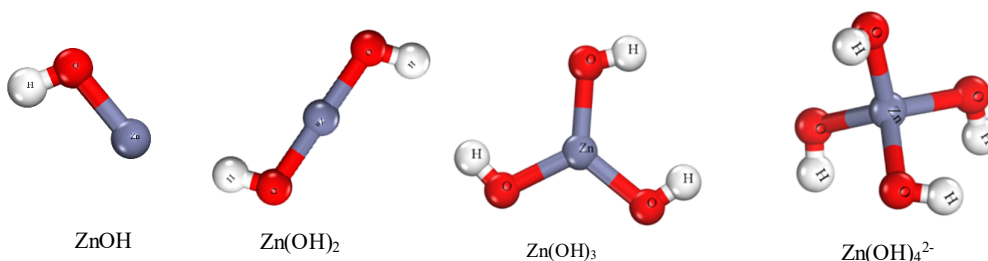


Figure 2. Optimized geometry of zinc hydroxide species.

The geometrical properties of zinc species from the chemistry viewpoint is really important. The chemical bond lengths between the H and O atoms in hydroxide ions were also investigated. The O-H

distances from ZnOH to Zn(OH)_4^{2-} were 0.985, 0.980, 0.974, and 0.979 Å, respectively. The results obtained indicate that the chemical bond length from ZnOH to Zn(OH)_3^- decreases, and there is a

little increase in more stable specie of $\text{Zn}(\text{OH})_4^{2-}$. Zinc and hydroxide ion bond lengths (ZnOH) in all molecular models increase by adding OH^- ions up to zincate. The measured average bond lengths based on Figure 1 models are 1.815, 1.827, 1.927, and 2.026 Å for ZnOH , $\text{Zn}(\text{OH})_2$, $\text{Zn}(\text{OH})_3^-$, $\text{Zn}(\text{OH})_4^{2-}$, respectively. It is clear that the bond length enhances slightly as ligand ion (OH^-) bonds increase. None of the models show a linear structure. In all models, zinc and oxygen have a single bond. There is a decreasing trend in the Zn-O-H bond angles except in ZnOH . The average Zn-O-H bond angles are 106.70, 108.15, 107.67, 103.30 degrees for ZnOH , $\text{Zn}(\text{OH})_2$, $\text{Zn}(\text{OH})_3^-$, and $\text{Zn}(\text{OH})_4^{2-}$, respectively. $\text{Zn}(\text{OH})_3^-$ and $\text{Zn}(\text{OH})_4^{2-}$ have trigonal and tetrahedral structures.

The O-Zn-O angles were measured after geometry optimization. The obtained values indicate no equal angles in each model. The average angles are 180, 178.70, 120, and 107.80 degrees for ZnOH , $\text{Zn}(\text{OH})_2$, $\text{Zn}(\text{OH})_3^-$, and $\text{Zn}(\text{OH})_4^{2-}$, respectively.

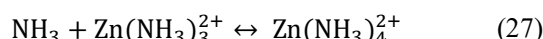
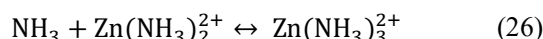
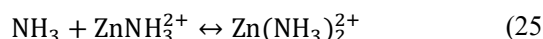
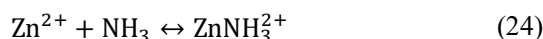
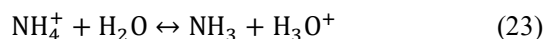
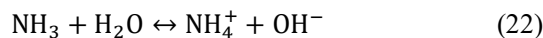
As Table 4 displays, the reaction free energies decrease by adding OH^- ions to the complexes. The reaction total free energy for reactions 4 and 1 were the lowest and the highest, respectively. The zincate speciation total free energy is -16.943 kcal/mol. The Spana simulations were validated by molecular modeling results with the decreasing trend in the reaction free energies. As shown in Table 4, the total reaction energies of Zn and OH^- are far more than zero, and prove that zinc hydroxide complexation occurs readily. A more negative reaction energy indicates that the reaction occurs more easily.

Table 4. Zinc hydroxide reaction energies in (kcal/mol).

Reaction	ΔG (kcal/mol)
$\text{Zn}^{2+} + \text{OH}^- \leftrightarrow \text{ZnOH}^+$	-30.12
$\text{ZnOH}^+ + \text{OH}^- \leftrightarrow \text{Zn}(\text{OH})_2$	-35.141
$\text{Zn}(\text{OH})_2 + \text{OH}^- \leftrightarrow \text{Zn}(\text{OH})_3^-$	-21.336
$\text{Zn}(\text{OH})_3^- + \text{OH}^- \leftrightarrow \text{Zn}(\text{OH})_4^{2-}$	-16.943

3.2. Zinc leaching mechanism by ammonia

The leaching mechanism of zinc oxide minerals with ammonia or ammonium salts is presented in this section. Figure 3 shows the Spana simulations of zinc ammine speciation in different Zn^{+2} concentrations. Based on the Spana simulations, the most stable zinc ammine species is $\text{Zn}(\text{NH}_3)_4^{2+}$. Reactions 22-27 show the proposed mechanism of $\text{Zn}(\text{NH}_3)_4^{2+}$ formation:



As Figure 3 shows in alkaline solution of ammonia and in all zinc concentrations and ammonia constant concentration, ZnNO_3^+ and ZnNO_2^+ can be formed at rarely similar thermodynamical conditions. It is clear that under certain conditions and decrease in zinc concentration but keeping the other conditions constant results in formation of $\text{Zn}(\text{NO}_2)_2$, specially in an acidic pH. Beside, the stability regions of $\text{Zn}(\text{NH}_3)_4^{2+}$ and $\text{Zn}(\text{OH})_4^{2-}$ increases by reduction of zinc concentration. Note that at a lower zinc concentration (b, c, d), $\text{Zn}(\text{NH}_3)_4^{2+}$ stability ranges are at $\text{pH} = 8.5-10$ and $\text{Eh} = -1-0$ but at a lower zinc concentration, $\text{Zn}(\text{NH}_3)_4^{2+}$ forms at a slightly lower $\text{pH} = 7-10$ and $\text{Eh} = -1-0$. Above $\text{pH} 12$, ammonia has no ability for complexation, and crystalline ZnO is stable. Obviously, at higher Eh ranges, the zinc ammine species are not stable. Based on these results, a higher concentration of ammonia is required to form stable $\text{Zn}(\text{NH}_3)_4^{2+}$.

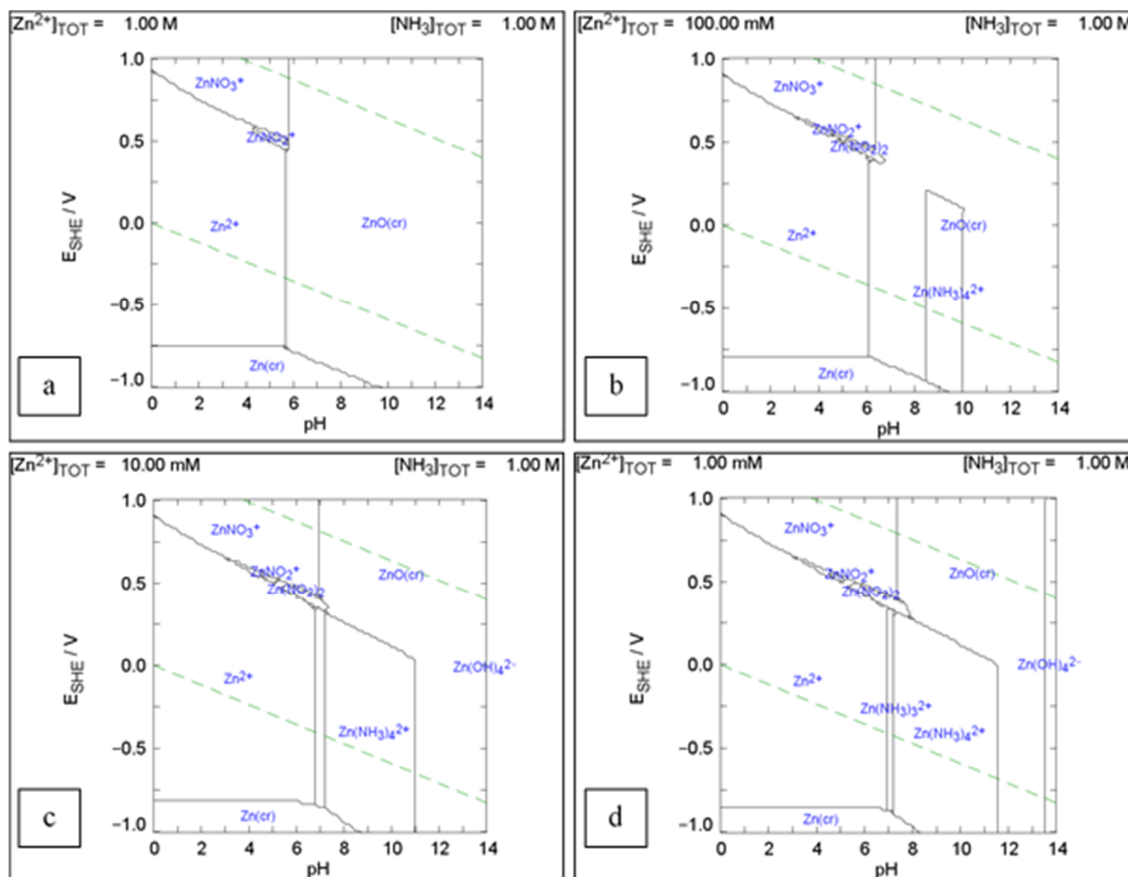


Figure 3. Zinc ammine speciation in 25 °C and 1.00 mol of Na⁺ (a) Zn²⁺ = 1 M, (b): Zn²⁺ = 100 mM, (c): Zn²⁺ = 10 Mm, and (d): Zn²⁺ = 1 Mm.

Figure 4 shows the optimized geometries of zinc ammine molecular models. The zinc and nitrogen bond lengths show that by ammonia adding, the length of the chemical bond increases. The Zn-N average bond lengths are 1.934, 1.925, 2.014, and 2.708 Å for Zn(NH₃)²⁺, Zn(NH₃)₂²⁺, Zn(NH₃)₃²⁺, and Zn(NH₃)₄²⁺, respectively. The N-Zn-N bond is linear (180 degrees) in model Zn(NH₃)₂²⁺ but non-linear in Zn(NH₃)₃²⁺ and Zn(NH₃)₄²⁺, making trigonal and tetragonal geometrical zinc ammine species. The model Zn(NH₃)₂²⁺ is rarely linear, and the average bond angles are 177.31, 120, and 109.471 degrees for Zn(NH₃)₂²⁺, Zn(NH₃)₃²⁺, and Zn(NH₃)₄²⁺, respectively.

The effect of complex orders on the NH₃ bond lengths (N-H) and bond angles (H-N-H) was investigated. In comparison between the highest

order complex of zinc ammine Zn(NH₃)₄²⁺ and free ammonia NH₃, the bond lengths are both 1.025 Å, similarly. There is no significant change in the first, second, and third order bond lengths as 1.03, 1.0325, and 1.0285, respectively.

Free ammonia has the lowest H-N-H bond angles (104.543 degrees) and the highest one is first order complex Zn(NH₃)²⁺ (109.384 degrees). The second, third, and fourth orders have similar bond angles but the third and fourth orders are very close as 107.655, 106.897, and 106.405 degrees, respectively. It is clear that the number of ligands (NH₃) have no significant effect on each other properties. Among all the ammine species, Zn(NH₃)₄²⁺ has more uniform geometric structure because of the same lengths of the bonds and similar bond angles.

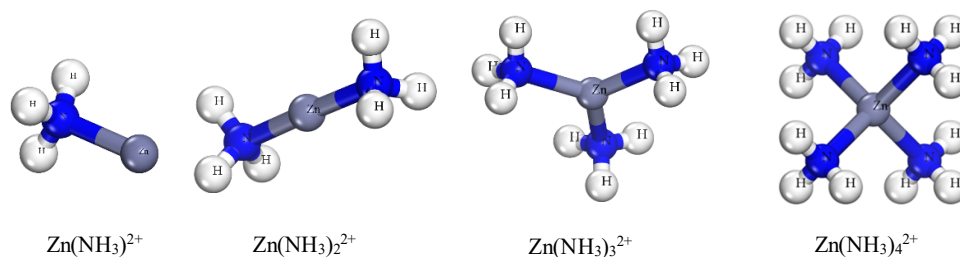


Figure 4. Optimized geometry of zinc ammine species.

Table 5 shows the zinc and ammonia reaction free energies. As it is shown, $\text{Zn(NH}_3\text{)}_4^{2+}$ has the lowest free energy in comparison with the other zinc ammine species. The zinc ammine species complexation total energy increases from ZnNH_3^{2+} to $\text{Zn(NH}_3\text{)}_4^{2+}$. The lowest total energy of zinc ammine complexation belongs to ZnNH_3^{2+} . The values obtained in this work show a sharp increase in the total energies by adding more NH_3 to the zinc ammine species.

Ligand addition to the structures have large effect on the reactants and reaction total free energies. As it is shown (Table 5) and based on the decreasing free energies of products, it can be concluded that the ligand high concentration is a very important factor, and favours formation of more stable complexes.

Table 5. Zinc ammine reaction energies in (kcal/mol).

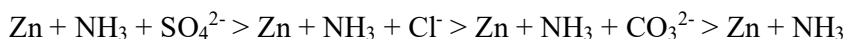
Reaction	ΔG (kcal/mol)
$\text{Zn}^{2+} + \text{NH}_3 \leftrightarrow \text{ZnNH}_3^{2+}$	-22.59
$\text{NH}_3 + \text{ZnNH}_3^{2+} \leftrightarrow \text{Zn(NH}_3\text{)}_2^{2+}$	-25.1
$\text{NH}_3 + \text{Zn(NH}_3\text{)}_2^{2+} \leftrightarrow \text{Zn(NH}_3\text{)}_3^{2+}$	-16.942
$\text{H}_3 + \text{Zn(NH}_3\text{)}_3^{2+} \leftrightarrow \text{Zn(NH}_3\text{)}_4^{2+}$	66.516

As the leaching process by alkaline reagents has a lower extraction than acidic leaching, in order to improve zinc dissolution, alternative ways like mechanical activation and adding ammonia salts

were used. In this section, the effect of the presence of ammonia salts in addition to ammonia that release anions in solution was investigated. The results obtained reveal the role of ammonia salts in leaching improvement.

Free energies of interaction of zinc, ammonia, and CO_3^{2-} , SO_4^{2-} , and Cl^- anions were calculated by molecular modeling. Figure 5 shows the optimized geometry structure of interacted zinc, ammonia, and anions. Changes in the interaction free energies completely reflect the effects of ammonia salts. The optimised geometries clearly show the tendency of nitrogen atom of ammonia to orient with the zinc atoms in the presence of other intermediates.

As Figure 5 shows, ammonia interaction with zinc in the presence of sulfate ion shifts toward a more negative value of interaction free energy compared with just ammonia and zinc. In other words, ammonium sulfate is more effective for zinc dissolution with ammonia, and leads to the formation of stronger species. This outcome signifies that in the presense of sulphate anion, adsorption of ligand on the zinc minerals surface occurs readily, and it reinforces the leaching process. Moreover, this finding confirmed the previous study results that ammonia salts improved the ammonia leaching process, and zinc dissolution increases. Based on Figure 5, free energies of species are in the following order:



Thus the reactivity of ammonia with zinc has a lower interaction energy than $\text{Zn} + \text{NH}_3 + \text{SO}_4^{2-}$. Consequently, these results indicate that addition

of ammonia salts favors the alkaline leaching of zinc oxides.

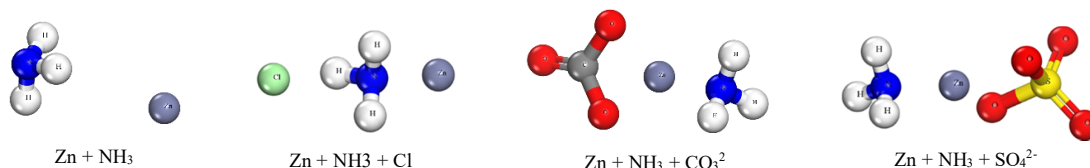


Figure 5. Interaction of ammonia salt anions with zinc.

In order to get more insight toward the interaction properties of zinc oxide minerals and alkaline agents, smithsonite mineral in the form of single cluster was investigated (Figure 6). Similar to the previous sections, Figure 6 demonstrates that the N and O atoms orient toward zinc atom in the smithsonite molecule. Table 6 indicates that OH^- ligand has a stronger interaction than NH_3 . The first

reaction shows -28.238 Kcal/mol interaction energy, similar to the Table 5 data. On the other hand, hydroxide ligand interaction energy is in good agreement with the Table 4 data.

The Zn-O and Zn-N distances are 1.848 and 1.977 angstrom, respectively. This could be attributed to the higher ability of hydroxide for complexation with zinc than ammonia.



Figure 6. Alkaline ligands interaction with Zn^{+2} .

Table 6. Smithsonite single cluster interaction with hydroxide and ammonia.

Interacting species	Interaction energy (kcal/mol)
Smithsonite + NH_3	-28.238
Smithsonite + OH^-	-36.396

4. Conclusions

According to the results obtained, it can be concluded that a higher concentration of alkaline ligands is required for zinc dissolution. In ammoniacal leaching, at lower pH and Eh, zinc dissolution and stable forms occur.

Molecular modeling showed that the zinc hydroxide species were more stable based on the higher reaction free energies. The reaction free energies indicate a downward trend in the complexation of zinc species to reach more stable species. $\text{Zn}(\text{NH}_3)_4^{2+}$ has the most regular structure among the other structures. The Zn-OH bonds are shorter than Zn- NH_3 , and ammine species show a more regular structure in comparison to the hydroxide structure, generally.

The change of free energies in the presence of ammoniacal salts indicate that sulfate ion (ammonium sulfate) is more effective in the stability. Thus the combination of ammonium sulfate and ammonia could result in improved dissolution, and a more stable species formation.

The smithsonite interaction with ammonia and hydroxide revealed that hydroxide led to a higher interaction energy than ammonia. This result is

consistent with the higher stability of hydroxide species. The results obtained revealed that Zn^{+2} reaction energy correlated well with the interaction energy of smithsonite single cluster model.

References

- [1]. Ju, S., Motang, T., Shenghai, Y. and Yingnian, L. (2005). Dissolution kinetics of smithsonite ore in ammonium chloride solution. *Hydrometallurgy*. 80 (1-2): 67-74.
- [2]. Ghasemi, S.M.S. and Azizi, A. (2018). Alkaline leaching of lead and zinc by sodium hydroxide: kinetics modeling. *Journal of materials research and technology*. 7 (2): 118-125.
- [3]. Frenay, J. (1985). Leaching of oxidized zinc ores in various media. *Hydrometallurgy*. 15 (2): 243-253.
- [4]. Abdel-Aal, E.A. (2000). Kinetics of sulfuric acid leaching of low-grade zinc silicate ore. *Hydrometallurgy*. 55 (3): 247-254.
- [5]. Espiari, S., Rashchi, F. and Sadrezhaad, S.K. (2006). Hydrometallurgical treatment of tailings with high zinc content. *Hydrometallurgy*. 82 (1-2): 54-62.
- [6]. Hurşit, M., Laçin, O. and Saraç, H. (2009). Dissolution kinetics of smithsonite ore as an alternative

zinc source with an organic leach reagent. *Journal of the Taiwan Institute of Chemical Engineers*. 40 (1): 6-12.

[7]. Larba, R., Boukerche, I., Alane, N., Habbache, N., Djerad, S. and Tifouti, L. (2013). Citric acid as an alternative lixiviant for zinc oxide dissolution. *Hydrometallurgy*, 134, 117-123.

[8]. Irannajad, M., Meshkini, M. and Azadmehr, A.R. (2013). Leaching of zinc from low grade oxide ore using organic acid. *Physicochemical Problems of Mineral Processing*. 49 (2): 547-555.

[9]. Chen, A., wei Zhao, Z., Jia, X., Long, S., Huo, G. and Chen, X. (2009). Alkaline leaching Zn and its concomitant metals from refractory hemimorphite zinc oxide ore. *Hydrometallurgy*. 97 (3-4): 228-232.

[10]. Moradkhani, D., Rasouli, M., Behnian, D., Arjmandfar, H. and Ashtari, P. (2012). Selective zinc alkaline leaching optimization and cadmium sponge recovery by electrowinning from cold filter cake (CFC) residue. *Hydrometallurgy*, 115, 84-92.

[11]. Kamran Haghighi, H., Moradkhani, D., Sardari, M.H. and Sedaghat, B. (2015). Production of zinc powder from Co-Zn plant residue using selective alkaline leaching followed by electrowinning. *Physicochemical Problems of Mineral Processing*, 51.

[12]. Lee, H.S. and Piron, D.L. (1995). Kinetics of alkaline leaching of pure zinc oxide. *Chemical Engineering Communications*. 138 (1): 127-143.

[13]. Ma, S.J., Yang, J.L., Wang, G.F., Mo, W. and Su, X.J. (2011). Alkaline leaching of low grade complex zinc oxide ore. In *Advanced Materials Research* (Vol. 158, pp. 12-17). Trans Tech Publications Ltd.

[14]. Habashi, F. (1993). A textbook of hydrometallurgy, metallurgie extractive Quebec. Enr. Que., Canada.

[15]. Ehsani, A., Ehsani, I. and Obut, A. (2021). Preparation of different zinc compounds from a smithsonite ore through ammonia leaching and subsequent heat treatment. *Physicochemical Problems of Mineral Processing*.

[16]. Soltani, F., Darabi, H., Aram, R. and Ghadiri, M. (2021). Leaching and solvent extraction purification of zinc from Mehdiabad complex oxide ore. *Scientific Reports*. 11 (1): 1-11.

[17]. Jiang, T., Meng, F.Y., Gao, W., Zeng, Y., Su, H.H., Li, Q. and Zhong, Q. (2021). Leaching behavior of zinc from crude zinc oxide dust in ammonia leaching. *Journal of Central South University*. 28 (9): 2711-2723.

[18]. Wang, R.X., Tang, M.T., Yang, S.H., Zhagn, W.H., Tang, C.B., He, J. and Yang, J.G. (2008). Leaching kinetics of low grade zinc oxide ore in $\text{NH}_3\text{-NH}_4\text{Cl-H}_2\text{O}$ system. *Journal of Central South University of Technology*. 15 (5): 679-683.

[19]. Yin, Z., Ding, Z., Hu, H., Liu, K. and Chen, Q. (2010). Dissolution of zinc silicate (hemimorphite) with

ammonia-ammonium chloride solution. *Hydrometallurgy*. 103 (1-4): 215-220.

[20]. Ding, Z., Yin, Z., Hu, H. and Chen, Q. (2010). Dissolution kinetics of zinc silicate (hemimorphite) in ammoniacal solution. *Hydrometallurgy*. 104 (2): 201-206.

[21]. Rao, S., Yang, T., Zhang, D., Liu, W., Chen, L., Hao, Z. and Wen, J. (2015). Leaching of low grade zinc oxide ores in $\text{NH}_4\text{Cl-NH}_3$ solutions with nitrilotriacetic acid as complexing agents. *Hydrometallurgy*. 158: 101-106.

[22]. Sinclair, R.J. (2005). The extractive metallurgy of zinc. Victoria: Australasian Institute of Mining and Metallurgy.

[23]. Liu, Z., Liu, Z., Li, Q., Yang, T. and Zhang, X. (2012). Leaching of hemimorphite in $\text{NH}_3\text{-(NH}_4\text{)2SO}_4\text{-H}_2\text{O}$ system and its mechanism. *Hydrometallurgy*, 125, 137-143.

[24]. Yang, K., Li, S.W., Zhang, L.B., Peng, J.H., Ma, A.Y. and Wang, B.B. (2016). Effects of sodium citrate on the ammonium sulfate recycled leaching of low-grade zinc oxide ores. *High Temperature Materials and Processes*. 35 (3): 275-281.

[25]. Yang, S.H., Hao, L.I., Sun, Y.W., Chen, Y.M., Tang, C.B. and Jing, H.E. (2016). Leaching kinetics of zinc silicate in ammonium chloride solution. *Transactions of Nonferrous Metals Society of China*. 26 (6): 1688-1695.

[26]. Liu, Z., Liu, Z., Li, Q., Cao, Z. and Yang, T. (2012). Dissolution behavior of willemite in the $\text{(NH}_4\text{)2SO}_4\text{-NH}_3\text{-H}_2\text{O}$ system. *Hydrometallurgy*, 125, 50-54.

[27]. Delley, B. (2000). From molecules to solids with the DMol 3 approach. *The Journal of chemical physics*. 113 (18): 7756-7764.

[28]. Klamt, A. and Schüürmann, G.J.G.J. (1993). COSMO: a new approach to dielectric screening in solvents with explicit expressions for the screening energy and its gradient. *Journal of the Chemical Society, Perkin Transactions 2*. (5): 799-805.

[29]. Hancock, R.D. and Bartolotti, L.J. (2005). Density functional theory-based prediction of the formation constants of complexes of ammonia in aqueous solution: Indications of the role of relativistic effects in the solution chemistry of gold (I). *Inorganic chemistry*. 44 (20): 7175-7183.

[30]. Gutten, O. and Rulisek, L. (2013). Predicting the stability constants of metal-ion complexes from first principles. *Inorganic Chemistry*. 52 (18): 10347-10355.

[31]. Yin, X., Opara, A., Du, H. and Miller, J.D. (2011). Molecular dynamics simulations of metal-cyanide complexes: Fundamental considerations in gold hydrometallurgy. *Hydrometallurgy*. 106 (1-2): 64-70.

مکانیزم تشکیل کمپلکس روی به وسیله لیگاندهای قلیایی: مطالعه مدل سازی مولکولی

داوود علوی، سیما محمدنژاد* و محمدجواد کلینی

بخش مهندسی معدن، دانشگاه تربیت مدرس، ایران

* نویسنده مسئول مکاتبات: sima.mnejad@modares.ac.ir

چکیده:

در این تحقیق، مکانیزم کمپلکس سازی هیدروکسید و آمونیوم روی در لیچینگ قلیایی و آمونیاکی به روش مدل سازی مولکولی و با روش تئوری تابع چگالی بررسی شده است. گونه شناسی کمپلکس های روی بر اساس داده های ترمودینامیکی و نمودارهای پوربه تعیین شد. ساختار واکنش دهنده ها به شکل کلاسترهای جداگانه با روش تئوری تابع چگالی مدل سازی شد. برای مقایسه ساختار گونه های هیدروکسید و آمین، مطالعات ساختاری نیز انجام شد. اثر نمک آمونیاک در بهبود و پایدارسازی گونه های آمین مطالعه گردید. برای فهم بهتر، اندرکنش تک مولکول های لیگاند با مولکول اسمیت زونیت نیز انجام شد. نتایج مدل سازی مولکولی نشان داد که گونه های هیدروکسیدی روی به دلیل انرژی آزاد منفی بالاتر پایدارتر هستند. انرژی واکنش با افزایش تعداد یون های OH^- و NH_3 در کمپلکس ها به ترتیب از $-30/12$ به $-16/943$ کیلوکالری بر مول و از $-22/590$ به $-66/516$ کیلوکالری بر مول کاهش یافت. پیوندهای Zn-OH کوتاه تر از Zn-NH_3 بوده و گونه های آمین ساختار منظم تری در مقایسه با ساختارهای هیدروکسیدی دارند. تغییر انرژی آزاد در حضور نمک های آمونیاکی معرف آن است که یونهای سولفات می توانند به طور قابل ملاحظه ای انحلال اکسید روی در آمونیاک را بهبود دهند. اندرکنش اسمیت زونیت با آمونیاک و هیدروکسید نشان می دهد یون های هیدروکسیدی منجر به انرژی اندرکنش بالاتری نسبت به آمونیاک ($-36/396$ در مقابل $-28/238$) شده که با پایداری بالاتر گونه های هیدروکسیدی مطابقت دارد. نتایج به دست آمده به خوبی نتایج آزمایشگاهی به دست آمده قبلی را توضیح داده و به طور مؤثری می تواند در بهینه سازی لیچینگ قلیایی کانستگ های اکسیدی روی مورد استفاده قرار گیرد.

کلمات کلیدی: اکسید روی؛ لیچینگ قلیایی؛ مدل سازی مولکولی؛ اسمیت زونیت؛ آمونیاک